Cellular Physiology and Biochemistry

Cell Physiol Biochem 2018;49:2264-2276
DOI: 10.1159/000493829
Published online: 27 September 2018
Accepted: 18 September 2018

Original Paper

Circular RNA Expression in the Brain of a Neonatal Rat Model of Periventricular White Matter Damage

Lihua Zhu[a] Ruibin Zhao[b] Li Huang[c] Sisi Mo[c] Zhangbin Yu[d] Li Jiang[c] Lixing Qiao[c]

[a]Institute of clinical, Jiangsu Health Vocational College, Nanjing, [b]Department of Pediatrics, Nanjing General Hospital, Nanjing, [c]Department of pediatrics, Zhongda hospital, Southeast University, District, Nanjing, [d]Department of Pediatrics, Nanjing Maternity and Child Health Care Hospital, Nanjing Medical University, Nanjing, China

Key Words
Circular RNA • Deep RNA sequencing • Periventricular white matter damage • Premature birth • Hypoxia-ischemia

Abstract
Background/Aims: Periventricular white matter damage (PWMD) is the predominant neurologic lesion in preterm infants who survive brain injury. In this study, we assessed the global changes in and characteristics of the transcriptome of circular RNAs (circRNAs) in the brain tissues of rats with PWMD. ***Methods:*** We compared the expression profiles of circRNAs in brain samples from three rats with PWMD and three paired control tissues using deep RNA sequencing. Bioinformatics analysis was applied to investigate these differentially expressed circRNAs, and quantitative reverse-transcription polymerase chain reaction (qRT-PCR) analysis was performed to confirm the results. Gene Ontology (GO) and Kyoto Encyclopedia of Genes and Genomes (KEGG) analyses were performed to predict associated cell signaling pathways and functions. Network analysis was performed to predict circRNAs-microRNAs, and target genes related to PWMD. ***Results:*** A total of 2151 more reliable circRNAs were dysregulated in the brain tissues of rats with PWMD, indicating a potential role in the condition. Of the 98 circRNAs significantly differentially expressed in rat brains with PWMD ($P < 0.05$), 52 were significantly over-expressed and 46 were significantly under-expressed. The expression profiles of seven of 10 randomly selected circRNAs were confirmed by qRT-PCR analysis. The glutamatergic synapse pathway and the VEGF signaling pathway, both associated with hypoxia/ischemia induced brain damage, were inriched. Relationship between miRNA (rno-miR-433-3p and rno-miR-206-3p) and HIF-1α were evident and potential associations between chr6:48820833|48857932 and their target genes (rno-miR-433-3p and rno-miR-206-3p) were

L. Zhu and R. Zhao contributed equally to this work.

Li Jiang
and Lixing Qiao

Department of Pediatrics, Zhongda Hospital, Southeast University
Nanjing210009, Jiangsu (China)
Tel. +86 25 83205301, E-Mail jiangli77777@126.com; qiaolixing@aliyun.com

identified. ***Conclusion:*** The distinct expression patterns of circRNAs in the brain tissues of rats with PWMD suggest that circRNAs actively respond to hypoxia-ischemia. These findings could assist the development of novel diagnostic and therapeutic targets for PWMD therapy.

Introduction

In premature infant, hypoxic-ischemic (HI) damage to cerebral white matter is a common and leading cause of brain injury that often results inchronic neurologic disability from cerebral palsy. During human brain development, between 23 and 32 weeks gestation, the periventricular cerebral white matter is at increased risk of injury from HI. HI, infection, inflammation, oxidative damage and excitotoxicity are pathogenic processes that collectively cause periventricular white matter damage (PWMD), and HI is believed to be a major factor in the evolution of PWMD [1].

Premature infants, particularly those with very low birth weight, brain injury are of enormous importance to public health because of the large numbers who survive the condition with serious neurodevelopmental disabilities, including major cognitive and behavioral defects [2, 3]. PWMD is the predominant neurologic lesion in preterm infants who survive brain injury [4, 5]. In China, approximately 1.5 million premature infants are born annually, among whom the incidence of PWMD is 5% [6]. Moreover, the proportion of premature infants has gradually increased over the past decade. Thus, the incidence of neurologic disability caused by premature birth can be expected to rise. Therefore, the discovery of new diagnostic biomarkers and therapeutic targets with the potential to control and predict the prognosis of PWMD is of great importance.

Imaging is an important method of diagnosing PWMD in premature infants. Craniocerebral ultrasound is employed as a screening tool for PWMD, and demonstrates high sensitivity and specificity for brain damage. Magnetic resonance imaging has a high resolution and shows the complete skull structure, however, it takes a long time to check, which is unacceptable for severely ill children. The lack of standardization of imaging examinations contributes to variation in diagnostic results between clinics. In addition, many factors can influence the accuracy of sonograph investigations for PWMD, such as the experience of operators, quality of the equipment, lesion type, and departmental policies and guidelines at individual institutions. Extraordinary diagnostic precision leading to low morbidity and mortality characterize state of the art clinical management of PWMD. When caring for a neonate with PWMD, it is critical to determine whether there is an underlying genetic element associated with the disease. Recent advancements in molecular biology techniques have facilitated the elucidation of the molecular mechanisms underlying brain formation, which involve microRNAs (miRNAs) [7], long noncoding RNAs (lncRNAs) [8] and circular RNAs (circRNAs) [9]. However, little is known about the role of circRNAs in the pathology of PWMD.

Recently deep sequencing and advanced data analysis techniques have enabled the characterization of thousands of circRNAs in multiple tissues and organisms. CircRNAs are a large class of non-coding RNA that exist ubiquitously in the cytoplasm of eukaryotic cells [10, 11]. In contrast to linear RNAs, circRNAs are single-stranded RNA molecules that form closed loops via covalent bonding [12] that have neither a 5'cap nor 3'tail, which may prevent degrdation by RNA exonuclease and thereby facilitate stable expression [13-15]. CircRNAs are mainly derive from the exonic regions of protein-coding genes, and are stable and varietyd in length. Endogenous circRNAs are thought to function as miRNA sponges, and are believed to antagonize miRNA-dependent gene regulation, thereby contributing to the competing endogenous RNA network [16]. In addition, circRNAs also regulate expressions of their parental genes. In Drosophila, circRNAs are most highly and specifically expressed in the brain [17]. This trend extends to mice and humans, suggesting that predominantly neural circRNA expression is conserved among species [13, 18, 19]. CircRNAs may have biologic roles relevant to the aging nervous system [20]. CircRNAs are widely involved in

physiologic/pathologic processes, including nervous system disorders [9, 18, 21], cancer [22-24], and pre-eclampsia [25]. Boeckel et al [26]. found that endothelial circRNAs are regulated by hypoxia and have distinct biological functions. In a stroke mouse model, circRNAs are implicated in the pathological development of brain injury [27]. CircRNAs are gaining attention in investigation on the mechanisms underlying disease and on biomarkers for disease diagnosis and treatment.

To examine the roles of circRNAs in the pathogenesis of PWMD, we performed sequence analysis to identify circRNAs that are differentially expressed in the brain tissues of rats with white matter damage, compared with control animals. We aimed to generate laboratory data for future clinical studies to assist the development of circRNA as potential biomarkers and diagnostic tools for premature infants with PWMD.

Materials and Methods

Animals

Two Pregnant Sprague-Dawley (SD) rats (day 18–19 of the estrous cycle) were obtained from Nanjing Medical University of China and allowed to deliver. All animals were treated appropriately according to the Guide for the Care and Use of Laboratory Animals (National Research Council). Experimental processes were approved by the Southeast University Animal Experimentation Committee. Pups were housed with their mother under a constant 12 h dark/ 12 h light cycle at 22°C ± 2°C with free access to food and water.

Neonatal Rat Model of Periventricular White Matter Damage

As described in our previous study [28], postnatal day 3 (P3) rats underwent permanent ligation of the right common carotid artery after anesthetization with ether. Pups were returned to the home cage for 2 h, then exposed to hypoxia (94% N2 + 6% O2) for 2h by being placed in a sealed chamber partially submersed in a 37°C water bath. At the end of the hypoxia treatment, pups were returned to their dam for recovery. In control rats, the same surgery was performed without ligation and exposure to hypoxia.

Brain Tissue Preparation

Rats were sacrificed with a lethal dose of pentobarbital (>50 mg/kg i.p.) at 24 h after operation. For hematoxylin and eosin (HE) staining (three control rats and three HI rats), brain tissues (3mm either side of the optic chiasm in the coronal plane) were removed after decapitation and fixed in 4% paraformaldehyde overnight at 4°C. For cryoprotection, brain tissue was transferred sequentially to 30% sucrose in 0.1 MPBS until it sank. Then embedded in O.C.T (Zhongshan Biotechnology Co., Ltd., Beijing, China) and stored at -80°C. Three control rats and three HI rats were used for sequencing, and six control rats and six HI rats were used for quantitative reverse-transcription polymerase chain reaction (qRT-PCR), the right brains were rapidly harvested, snap frozen in liquid nitrogen and kept at −80°C.

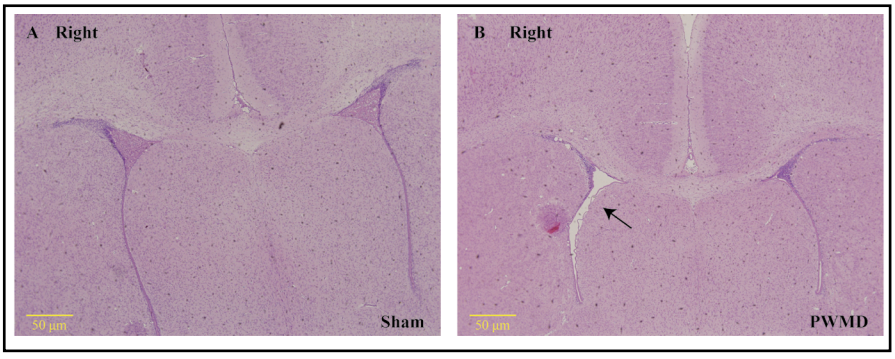

Fig. 1. HE stained coronal brain sections. (A) The white matter under the cortex and corpus callosum appeared normal in sham rats. (B) In rats with PWMD, the right white matter exhibited leukoaraiosis, and the right ventricle appeared expanded (arrow).

Hematoxylin and Eosin (HE) Staining

Consecutive frozen brain sections were used for HE staining. The HE stained sections were examined under the microscope for any alteration in histopathology. Slides were examined with a computer-assisted Olympus CK_2 microscope. Five sections from each rat were taken from the right white matter region. In the right brain of HI rats, the white matter under the cortex and corpus callosum exhibited serious leukoaraiosis, ventricles were expanded, the arrangement of neurons in the gray matter was disordered, and apoptosis was evident (Fig. 1).

Whole Transcriptome Library Preparation

Total RNA was obtained using TRIzol (Invitrogen, UK) according to the manufacturer's protocol. Total genomic DNA was then removed from RNA samples using DNase I (NewEngland Biolabs) and RNA purity was assessed using a Nanodrop-2000 instrument. Each RNA sample had an A260:A280 ratio above 1.9 and an A260:A230 ratio above 1.8. Total RNA was subject to ribosomal RNA depletion according to the manufacturer's protocol supplied with the Ribo-Minus kit (Life Technology). Next, RNA was fragmented into 200~300 base pairs (bp) using an RNA fragmentation kit (Ambion) and quantified with Nanodrop instrument (Thermo Scientific). The first cDNA strand was synthesized using random hexamer primers, and the second strand cDNA was synthesized using dUTP instead of dTTP. In this step, actinomycin D was used to increase strand specificity by inhibiting second-strand cDNA synthesis. At 15°C 0.5μl of actinomycin D solution (120 ng/μl), 0.5 μl of RNase OUT (40 units/μl, Invitrogen) and 0.5 μl of SuperScript III polymerase (200 units/μl, Invitrogen) were added to the reaction. Then, EB (20μl) (10mM Tris–Cl, pH 8.5, Qiagen) was added and the dNTPs were removed by purification of the first strand mixture using a 200μl G-50 gel filtration spin-column equilibrated with 1mM Tris–Cl, pH 7.0. After second strand synthesis and DNA fragmentation, sequencing libraries were constructed by following the manufacturer's instructions (Illumina). Fragments of 300-400 bp were recovered and purified, then enriched by 15 cycles of PCR. Each library was loaded into one lane of an Illumina HiSeq 2500 for 2×150 bp pair-end（PE）sequencing.

Deep RNA sequencing (RNA-seq)

We used FastQC (http://www.bioinformatics.babraham.ac.uk/projectissue specific/fastqc/) to control the quality of the sequencing data. At an initial filtering step, we discarded low quality reads, including reads that had adaptors, reads with ≥ 10% unknown bases, and reads that had ≥ 50% bases with a quality value ≤ 5.

Next, we applied CIRI [29] to identify circRNAs. For the CIRI algorithm, we first mapped the filtered data to the *Rattus_norvegicus*.Rnor_6.0 genome reference using BWA [30] software. Based on the Sequence Alignment Map file, CIRI was used to detect circRNAs.

To ensure the accuracy of circRNA identification, we retained only high-confidence circRNAs by adopting two criteria: selecting circRNAs identified in at least two junction reads; and selecting circRNAs present in more than four samples.

To obtain the full-length nucleotide sequence of all circRNA isoforms, we compared the back-spliced junction sites with the Rattus_norvegicus.Rnor_6.0 genome annotation downloaded from UCSC [31] database. Reportedly, multiple circRNA isoforms can be generated from the same back-spliced junction site [32, 33]. Based on the method of Liu et al [34]., we identified multiple circRNA isoforms with annotated transcripts if the "head" and "tail" positions of the detected back-spliced junction were located exactly at exon junction sites or if part of the junction sites had small flanking portions of intron sequencing. We also identified some circRNA isoforms associated with their back-spliced junction sites located in intergenic regions, with no overlap with known genes or overlap with known genes but localized on their antisense strands. CircRNAs that were fully located in intronic regions were also retained. CircRNAs obtained from each sample were filtered (standard: junction reads≥2), and all circRNAs present in more than four samples were collated. To assess differentially expressed circRNAs, raw counts of reads spanning a particular head-to-tail junction were analyzed using edgeR package (version 3.12.1) with TMM normalization in generalized linear model. The Trimmed Mean of M-values (TMM) normalization method was used to minimize size bias between samples for sequencing libraries. Significantly differentially expressed circRNAs were those exhibiting a fold change (FC) ≥1.5 and P-value < 0.05. All statistical analyses were performed using R 3.2.3 (http://www.r-project.org/).

Confirmation of CircRNA Expression via Quantitative Real-Time Polymerase Chain Reaction (qRT-PCR) Analysis

Ten circRNAs we selected for qRT -PCR analysis based on the following conditions; (1) statistically significant differences between control and PWMD groups in the RNA-Seq analysis; (2) relatively high expression; (3) the host gene was normal in HI-induced brain damage. Total RNA was isolated from neonatal rat brains using TRIzol reagent (Invitrogen, UK) according to the manufacturer's protocol. The purity and concentration of RNA were evaluated by measuring the OD260/280 ratio in a spectrophotometer. Total RNA was reverse transcribed using a PrimeScript™ RT reagent kit (Takara, Otsu, Shiga, Japan). After cDNA synthesis, real-time PCR was performed using SYBR Premix Ex Taq™ (Takara) for amplification of the PCR products. The β-actin gene was chosen as a reference gene. All reactions were performed in triplicate with the same cDNA samples. The final results were expressed as the relative expression ratio between the targeted gene and the β-actin reference gene. Relative gene expression was analyzed using the $2^{-\Delta\Delta Ct}$ method. Primer information is listed in Table 1.

Table 1. Sequences of primers for the internal reference gene and circRNAs. F:Forward; R:Reverse; PS: Product size

Primer	5´-3´ (sense)	PS(bp)
β-actin	F:CTGAACCCTAAGGCCAACC R:AGCGCGTAACCCTCATAGAT	250
chr1:17536371|17554677	F:TCAACGCCTTCATAGTCAG R:GGACCACCTACCAGTTCTTC	118
chr18:24611733|24614740	F:TCTCATCCGCTTCCC R:ATGCCGAGGTTCCAG	108
chr18:73479863|73498648	F:TGAAGCAGCACAGAAGC R:AGACGCCGATACCCAC	188
chr7:114487838|114499158	F:AAGGCTGTAGAGGGTGG R:TGTGGGAGATACTGATGC	128
chr2:41261840|41286354	F:CTGGCAATCGAGGAGTT R:TGGACAATGGCACATCA	178
chr15:837322|852690	F:GGCTATGAAACCCAACT R:AGAACTACCACCCAAAGAT	143
chr7:30727478|30735182	F:CTTCTGAGACGGGTGC R:AAGGTGGATGTGGTGC	108
chr14:9421418|9440942	F:AGGTCGTAGGAGTGGTAGA R:TGGAAGAACTGGTGGATT	170
chr6:48820833|48857932	F:TTCTCCTCCTCAATCGT R:ATCAAGCAGCGAGCC	140
chr16:63915078|63933482	F:CTGGGTGAAACGAGC R:TTGAAACAACGGCAAC	132

Bioinformatics analysis

We performed Gene Ontology (GO) and Kyoto Encyclopedia of Genes and Genomes (KEGG) enrichment analyses of the parent genes of all specific differentially expressed circRNAs, and removed duplicate genes using DAVID v6.7 [35, 36]. KEGG pathway enrichment analysis was performed using the KEGG Orthology Based Annotation System (KOBAS 3.0, http://kobas.cbi.pku.edu.cn/anno_iden.php) [37].

We selected specific circRNAs and construct a network according to the circRNA profiling data. CircRNA-miRNA interaction were predicted using Arraystar miRNA target prediction software based on TargetScan and miRanda [27, 38], and miRNA-mRNA interactions were predicted using miRTarBase [27].

Statistical Analysis

All data in this article are expressed as means ±standard deviation. Graphs were generated using Microsoft Excel (Microsoft Corp., Redmond,WA, USA). Statistical analysis was performed using SPSS 18.0 (SPSS Inc., Chicago,IL, USA). Differences between the two groups were determined using the independent-samples t-test. Probability levels of 0.05 were considered statistically significant.

Results

Results of Deep RNA Sequencing

We predicted 2151 probable circRNAs. Based on the circRNA expression profiles, differentially expressed circRNAs were identified in the PWMD group compared with the sham group. Hierarchical clustering was performed to group circRNAs based on their expression levels (Fig. 2A). We set a threshold of a fold change >1.5 and a p-value <0.05. We found that 98 circRNAs were differentially expressed in the PWMD group (Fig. 2B and 2C), of which the top 40 are listed in Table 2. Of them, 52 were significantly over-expressed and 46 were significantly under-expressed. Among the up-regulated circRNAs, 13 were intergenic, one was intronic, and 38 were exonic. Among the down-regulated circRNAs, seven were intergenic, one was intronic, and 38 were exonic (Fig. 2D).

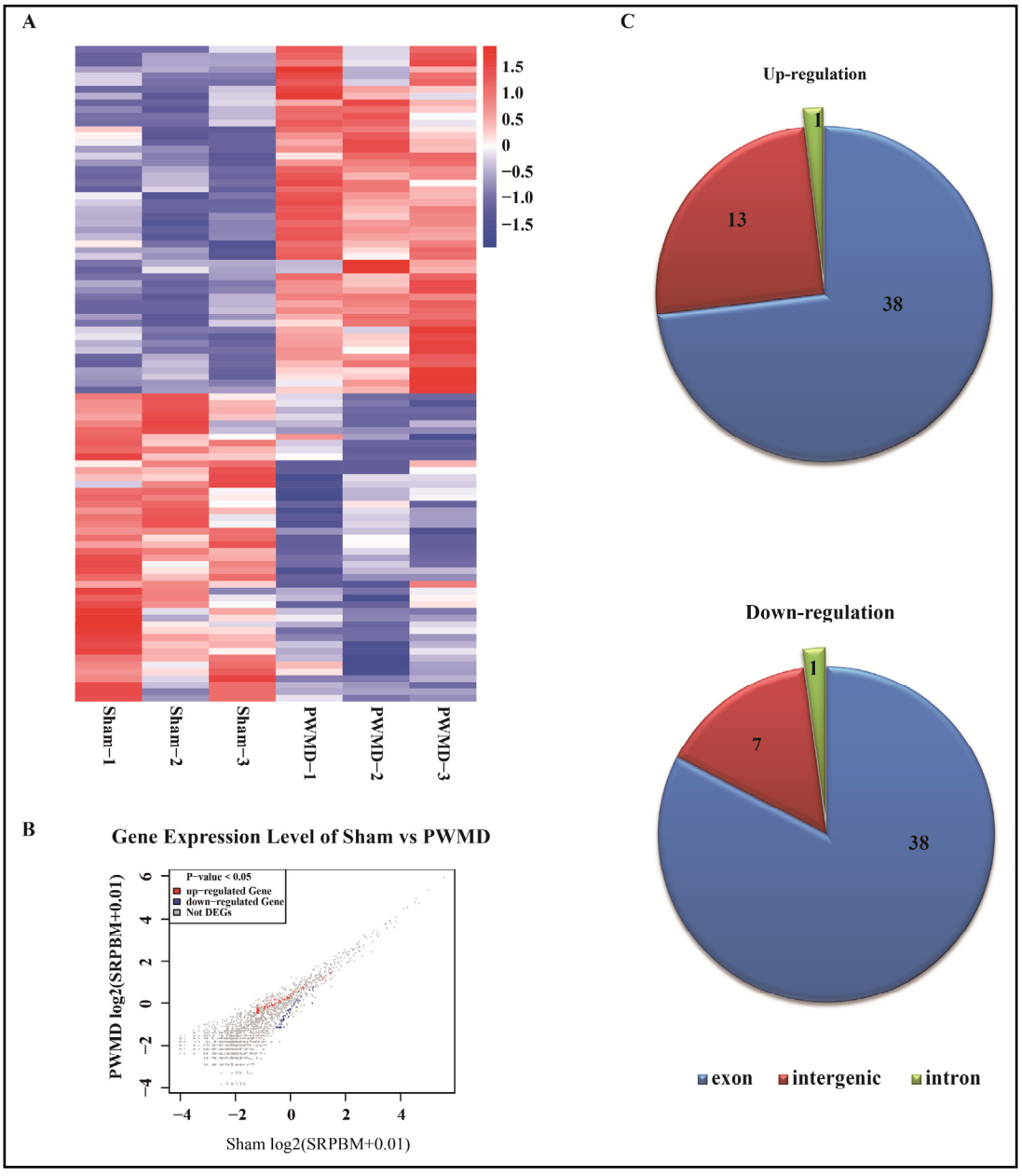

Fig. 2. Analysis of differentially expressed circRNAs. (A) The hierarchical clustering of partial differentially expressed circRNAs. 'Red' indicates high relative expression, and 'blue' indicates low relative expression. (B) CircRNAs in the Scatter-Plot. 'Red' indicates up-regulation and 'blue' indicates down-regulation more than 1.5 fold change of circRNAs between the two groups. (C) Classification of dysregulated 1.5-fold up and down expressed circRNAs with statistical significance (P<0.05).

Validation of CircRNA Expression

We randomly selected 10 circRNAs, including four up-regulated circRNAs (chr1:17536371|17554677, chr2:41261840|41286354, chr15:837322|852690, and chr14:9421418|9440942) and six down-regulated circRNAs (chr18:24611733|24614740, chr18:73479863|73498648, chr7:114487838|114499158, chr7:30727478|30735182, chr6:48820833|48857932, and chr16:63915078|63933482) for verification by qRT-PCR analysis. A general consistency was evident between the real-time PCR and RNA-seq results. The expression of two of the selected up-regulated circRNAs (chr1:17536371|17554677

and chr15:837322|852690), five of the selected down-regulated circRNAs (chr18:24611733|24614740, chr7:114487838|114499158, chr6:48820833|48857932 and chr16:63915078|63933482, *P* <0.01) (chr18:73479863|73498648, *P* <0.05) were confirmed (Fig. 3). There wasere no significant differences for chr7:30727478|30735182 (*P*=0.31) or chr14:9421418|9440942 (*P*=0.619) between two groups by qRT-PCR analysis. However, the expression trends of both were consistent with those determined using RNA-seq. The expression trend of chr2:41261840|41286354 was not confirmed.

Gene Ontology and KEGG Enrichment Analysis

Under the assumption that the function of circRNAs is related to the known function of the host genes, we performed GO enrichment and KEGG pathway analyses to predict the potential functions of deregulated circRNAs.

GO enrichment analysis suggested that the host genes of PWMD specific circRNAs were of several functional categories. Highly enriched GO terms associated with circRNA transcripts among biological process, cellular components, and molecular functions are shown in Table 3. KEGG enrichment analysis

Table 2. Top 40 differentially expressed circRNAs between PWMD and sham groups. FDR, false discover rate; FC, fold change. The circular RNAs identified to be dysregulation by P value <0.05

circRNA	P-value	FDR	FC	Regulation	circRNA type	Gene Symbol
chr1:17536371|17554677	0.000	0.062	9.879	up	exon	Ptprk
chr14:86326421|86326743	0.001	0.347	7.513	up	exon	Nudcd3
chr3:29584278|29597359	0.006	0.630	6.713	up	intron	Gtdc1
chr15:837322|852690	0.015	0.782	6.428	up	exon	Kcnma1
chr9:50892486|50906966	0.016	0.782	6.379	up	intergenic	-
chr6:14450092|14758647	0.015	0.782	6.331	up	intergenic	-
chr6:30550488|30589369	0.001	0.352	6.297	up	intergenic	-
chr7:126265888|126283984	0.014	0.782	6.003	up	exon	Atxn10
chr5:94693114|95108520	0.015	0.782	5.939	up	intergenic	-
chr14:9421418|9440942	0.024	0.903	5.619	up	exon	Cds1
chr4:34740521|34761519	0.038	0.963	5.607	up	exon	Ica1
chr6:7718824|7738462	0.006	0.630	5.600	up	exon	Thada
chr1:241731334|241732616	0.047	0.963	5.598	up	exon	Apba1
chr1:175200414|175218889	0.020	0.889	5.221	up	exon	Sbf2
chr1:157470071|157490006	0.046	0.963	4.860	up	exon	Pcf11
chr19:38057557|38062193	0.005	0.610	4.690	up	exon	Nfatc3
chr2:116586880|116594945	0.000	0.126	4.620	up	intergenic	-
chr1:119172338|119555633	0.011	0.761	4.542	up	intergenic	-
chr16:39881896|39884207	0.047	0.963	4.454	up	exon	Wdr17
chr3:92183759|92225505	0.047	0.963	4.453	up	exon	Trim44
chr18:24611733|24614740	0.000	0.126	9.786	down	exon	Wdr33
chr11:83225853|83225993	0.002	0.359	8.241	down	intron	Vps8
chr12:39627016|39635912	0.003	0.466	7.435	down	exon	Anapc7
chr14:28418126|28465972	0.008	0.722	7.384	down	exon	Adgrl3
chr7:114487838|114499158	0.009	0.734	7.062	down	exon	Ptk2
chr18:73479863|73498648	0.009	0.722	6.557	down	exon	Pias2
chr9:118986481|118991497	0.009	0.722	6.543	down	exon	Dlgap1
chr13:97559165|97566714	0.040	0.963	5.632	down	intergenic	-
chr10:74338952|74360926	0.008	0.722	5.538	down	exon	Gdpd1
chr18:13369444|13417002	0.044	0.963	5.180	down	intergenic	-
chr4:182811463|182826795	0.045	0.963	5.168	down	exon	Tmtc1
chr16:54054981|54061837	0.046	0.963	5.156	down	exon	Pcm1
chr3:15042229|15042609	0.041	0.963	4.650	down	exon	Dab2ip
chr3:21850499|21878612	0.001	0.279	4.644	down	exon	Strbp
chr2:195751903|195795666	0.044	0.963	4.623	down	exon	Snx27
chr18:5191058|5194413	0.034	0.963	4.382	down	exon	Zfp521
chr7:124682871|124727275	0.004	0.527	4.314	down	exon	Mpped1
chr15:34277381|34277914	0.013	0.782	4.140	down	exon	Rnf31
chr1:195625166|195866944	0.039	0.963	3.956	down	intergenic	-
chr14:81163989|81182711	0.024	0.903	3.730	down	exon	Htt

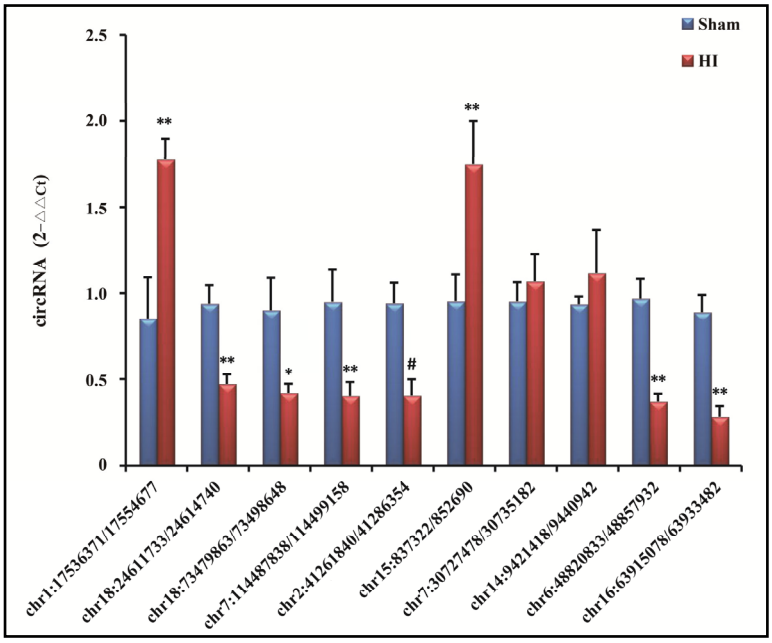

Fig. 3. Validation of ten circRNAs expression by qRT-PCR. The values shown are the means ±standard deviation. ** means P<0.01 vs. the sham group, * means P<0.05 vs. the sham group, and the expressions were consistent between sequencing and real-time PCR. # means P<0.01 vs. the sham group, but the expressions were inconsistent between sequencing and real-time PCR. No sign means of P > 0.05 vs. the sham group, however consistent with the trend of sequencing.

revealed that the host genes of circRNAs were enriched in some PWMD function related pathways. One of the most enriched signaling pathways was the glutamatergic synapse pathway, and the vascular endothelial growth factor (VEGF) signaling pathway was also enriched (Table 4). Interesting, both of these pathway arereportedly involved in HI induced brain damage [39, 40].

Prediction of CircRNAs/ miRNAs and Target Genes

Recent studies have reported that circRNAs can function as miRNA sponges to modulate miRNA expression and miRNA-dependent gene regulation [13, 16, 41]. This interaction between circRNAs and disease-associated miRNAs suggests that circRNAs function in disease regulation [16, 21, 41]. Two confirmed circRNAs (chr6:48820833|48857932 and chr16:63915078|63933482) and two circRNAs (chr7:30727478|30735182 andchr14:9421418|9440942) for which the expression trends were consistent with RNA-seq data were annotated in detail using circRNA-miRNA interaction information. The potential miRNA targets of circRNAs and mRNA targets of miRNA list in Supplementary Fig. S1 (For all supplementary material see www.karger.com/10.1159/000493829/). Most of the identified circRNAs contain one or more miRNA binding sites, and some appear to bind tightly to one miRNA via multiple sites. For example, rno-miR-216a-5p is strongly complementary to three circRNAs

Table 3. Significantly enriched GO terms for differentially expressed circRNA genes between PWMD and sham groups

Category	Name	Count	P-value
Molecular-function	protein binding	18	0.000
Molecular-function	protein domain specific binding	8	0.000
Molecular-function	phosphatidylinositol 3-kinase binding	3	0.004
Molecular-function	zinc ion binding	11	0.005
Molecular-function	identical protein binding	8	0.010
Molecular-function	ion channel binding	4	0.012
Molecular-function	protein complex binding	6	0.012
Molecular-function	protein kinase binding	6	0.024
Molecular-function	metal ion binding	11	0.033
Cellular-component	cytosol	19	0.000
Cellular-component	postsynaptic density	7	0.000
Cellular-component	axon	8	0.000
Cellular-component	dendrite	9	0.000
Cellular-component	synapse	7	0.000
Cellular-component	neuronal cell body	9	0.000
Cellular-component	cytoplasm	32	0.002
Cellular-component	cell junction	6	0.018
Cellular-component	nucleoplasm	13	0.026
Cellular-component	membrane	15	0.030
Cellular-component	postsynaptic membrane	4	0.037
Biological-process	brain development	7	0.000
Biological-process	regulation of GTPase activity	4	0.001
Biological-process	neuron projection development	5	0.002
Biological-process	intracellular protein transport	5	0.007
Biological-process	positive regulation of neuron projection development	4	0.015
Biological-process	positive regulation of protein kinase activity	3	0.020
Biological-process	regulation of ion homeostasis	2	0.022
Biological-process	positive regulation of phosphatidylinositol 3-kinase signaling	3	0.023
Biological-process	positive regulation of ion transmembrane transporter activity	2	0.025
Biological-process	chemical synaptic transmission	4	0.026
Biological-process	protein autophosphorylation	4	0.031
Biological-process	positive regulation of axon regeneration	2	0.036
Biological-process	nervous system development	4	0.037
Biological-process	positive regulation of protein kinase B signaling	3	0.039

Table 4. KEGG Pathway for differentially expressed circRNAs between PWMD and sham groups

Term	ID	P-value	Input gene
Glutamatergic synapse	rno04724	0.000	Prkcb;Grik2;Ppp3cc;Dlgap1
VEGF signaling pathway	rno04370	0.001	Prkcb;Ppp3cc;Ptk2
Ubiquitin mediated proteolysis	rno04120	0.001	Pias2;Anapc7;Trip12;Herc1
ErbB signaling pathway	rno04012	0.004	Prkcb;Ptk2;Nrg
Ras signaling pathway	rno04014	0.009	Prkcb;Tiam1;Ksr2;Igf1r
Amino sugar and nucleotide sugar metabolism	rno00520	0.013	Uxs1;Cyb5r4
Wnt signaling pathway	rno04310	0.015	Prkcb;Nfatc3;Ppp3cc
Long-term depression	rno04730	0.020	Prkcb;Igf1r
Long-term potentiation	rno04720	0.021	Prkcb;Ppp3cc
cGMP-PKG signaling pathway	rno04022	0.021	Kcnma1;Nfatc3;Ppp3cc
Axon guidance	rno04360	0.026	Ptk2;Nfatc3;Ppp3cc
Chemokine signaling pathway	rno04062	0.026	Prkcb;Tiam1;Ptk2
Focal adhesion	rno04510	0.034	Prkcb;Ptk2;Igf1r
Rap1 signaling pathway	rno04015	0.039	Prkcb;Tiam1;Igf1r
Regulation of actin cytoskeleton	rno04810	0.040	Tiam1;Ptk2;Iqgap2
Phosphatidylinositol signaling system	rno04070	0.046	Prkcb;Cds1
Natural killer cell mediated cytotoxicity	rno04650	0.047	Prkcb;Ppp3cc
Retrograde endocannabinoid signaling	rno04723	0.054	Prkcb;Rims1
HIF-1 signaling pathway	rno04066	0.055	Prkcb;Igf1r
T cell receptor signaling pathway	rno04660	0.059	Nfatc3;Ppp3cc
MAPK signaling pathway	rno04010	0.065	Prkcb;Nfatc3;Ppp3cc
Vascular smooth muscle contraction	rno04270	0.066	Prkcb;Kcnma1
Dopaminergic synapse	rno04728	0.077	Prkcb;Ppp3cc
mTOR signaling pathway	rno04150	0.111	Prkcb;Igf1r
Calcium signaling pathway	rno04020	0.131	Prkcb;Ppp3cc
Carbohydrate digestion and absorption	rno04973	0.135	Prkcb
cAMP signaling pathway	rno04024	0.153	Tiam1;Pde4d
Synaptic vesicle cycle	rno04721	0.193	Rims1
GABAergic synapse	rno04727	0.277	Prkcb
NF-kappa B signaling pathway	rno04064	0.280	Prkcb
PI3K-Akt signaling pathway	rno04151	0.321	Ptk2;Igf1r
Cholinergic synapse	rno04725	0.326	Prkcb
Serotonergic synapse	rno04726	0.353	Prkcb
Sphingolipid signaling pathway	rno04071	0.357	Prkcb
AMPK signaling pathway	rno04152	0.367	Igf1r
FoxO signaling pathway	rno04068	0.369	Igf1r
Apoptosis	rno04210	0.383	Dab2ip
Tight junction	rno04530	0.389	Prkcb
Jak-STAT signaling pathway	rno04630	0.418	Pias2
Protein processing in endoplasmic reticulum	rno04141	0.443	Ubqln1
Alzheimer's disease	rno05010	0.451	Ppp3cc
Purine metabolism	rno00230	0.469	Pde4d
Endocytosis	rno04144	0.620	Igf1r
Neuroactive ligand-receptor interaction	rno04080	0.634	Grik2

(chr7:30727478|30735182, chr6:48820833|48857932 and chr16:63915078|63933482). We then examined the mRNA binding results and found that chr6:48820833|48857932 and chr16:63915078|63933482 can bind to the miRNA effector pten. We also identified potential associations between chr6:48820833|48857932 and their target genes (rno-miR-433-3p and rno-miR-206-3p), and potential relationships between miRNA rno-miR-433-3p and HIF-1α, rno-miR-206-3p, and HIF-1α.

Discussion

In this study, we examined the transcriptome of circRNAs in a neonatal rat model of PWMD. This study is the first to profile circRNAs differentially expressed in rats with PWMD compared with healthy rats.

CircRNAs are non-coding RNAs (ncRNAs) produced in eukaryotic cells during post-transcriptional processes. Recent studies have revealed that circRNAs are primarily generated from exons or introns of their parental genes [13, 42, 43] and can regulate the expression of parental genes [44-46]. Many exonic transcripts can form circRNAs through non-linear reverse splicing or gene rearrangement. CircRNAs can potentially regulate multiple aspects of cellular physiology, including miRNA binding, translational regulation, protein interactions, and even protein translation. RNA-seq of transcripts showed that, in the brain, a significantly greater fraction of reads are circRNA junction reads, a greater number of genes are hosts to circRNAs, and there are many tissue-specific circRNA hosts [47]. CircRNAs contain highly conserved sequences and display a high degree of stability in mammalian cells [18]. These properties mean that circRNAs have the potential to be used as stable biomarkers and potential therapeutic targets [48].

In this study, we chose RNA-seq to identify circRNAs. Microarray analysis is the most popular technology for the investigation of global RNA expression, involving probes designed to recognize annotated genes or sequences present in the genome. However, microarray analysis cannot detect undiscovered circRNAs. By contrast, RNA-seq can, in principle, detect any expressed RNAs and identify "aberrant" junction sequences, thereby signaling the presence of circRNAs [49]. In this study, we predicted 2151 probable circRNAs in silico, and selected circRNAs that co-occurred in more than four samples for further analysis. Thus, the true number of circRNAs is certainly much larger.

A recent evaluation of five different circRNA prediction algorithms found dramatic differences between their outputs, emphasizing that these prediction results should be handled with care [50]. Therefore, for any candidate circRNA identified, further independent experimental validation is required [51]. In this study, we validated the expression of 10 circRNAs using qRT-PCR. As a result, the expression of two up-regulated circRNAs and five down-regulated circRNAs was confirmed. Although there was no significant difference in the expression of circRNAs chr7:30727478|30735182 and chr14:9421418|9440942 between the two groups according to qRT-PCR analysis, their expression trends were consistent with those detected by RNA-seq. Increasing the number of samples may yield clearer results. However, this validity is consistent with that of other studies [52]. At the time of writing, these circular RNAs had not been identified in other studies using similar samples.

To investigate the functions of these PWMD specific circRNAs, we performed GO enrichment and KEGG pathway analyses of their annotated host protein coding genes. GO enrichment analyses revealed that some genes were involved in the regulation of biological processes, cellular components, and molecular functions. Signaling pathways such as the glutamatergic synapse pathway and VEGF pathway are reportedly associated with HI induced brain injury. Liu et al [39]. found that the thalamocortical circuitry is affected and vulnerable in PWMD mice and glutamatergic synaptic transmission is associated with such changes. Meanwhile, VEGF signaling pathway is involved in anoxia in rats, and recombinant human erythropoietin promotes brain recovery through this pathway [40]. These results showed that these genes generate one or more specifically expressed circRNAs, suggesting

that these PWMD specific circRNAs play important roles in the molecular basis of phenotype heterogeneity in neonates with PWMD.

CircRNAs can function as a miRNA sponges, and may alleviate the inhibitory effects of miRNAs on target molecules, thereby regulating gene expression. Reportedly, the antisense sequence of cerebellar degeneration-related protein1 transcript (CDR1as) is a representative molecular sponge. CDR1as contains approximately 74 binding sites for miR-7, and CDR1as over-expression down-regulates miR-7 expression [18, 53]. In this study, we identified many dysregulated circRNAs in the brains of rats with PWMD. We found that most of the circRNAs contained one or more miRNA binding sites. We found that some circRNAs could bind densely to one miRNA. Therefore, we deduced that circRNAs probably compete with other RNAs for miRNA binding. HIF-1α is a member of the Hypoxia Inducible Factor (HIF) family. Endogenous hypoxia-inducible mechanisms are crucial during the early stages of brain development. Hypoxia appears to activate mitogen-activated protein kinase that phosphorylates HIF-1α and thereby stabilizes the molecule. In the neonatal brain, when hypoxia is accompanied by ischemia there are more persistent alterations of HIF-1α expression. To date, more than 100 target genes of HIF-1α have been identified with varying functions, including erythropoiesis/iron metabolism, angiogenesis, vascular tone, matrix metabolism, glucose metabolism, cell proliferation/survival, necrosis, anti-apoptosis and apoptosis [54]. We found that HIF-1α was significantly altered in the brain tissue of neonatal rats after hypoxic ischemia [55]. This network indicated a targeted relationship between miRNA (rno-miR-433-3p and rno-miR-206-3p) and HIF-1α, and potential associations between chr6:48820833|48857932 and their target genes (rno-miR-433-3p and rno-miR-206-3p). This may represent one of the key mechanisms in PWMD. To date, a clear function has only been demonstrated for a few circRNAs that serve as miRNA sponges [13, 16, 56], sequestering miRNAs and preventing their interactions with target mRNAs. Further analysis is warranted to prove that these circRNAs act as a miRNA sponges.

There are some limitations of the present study. First, translating these findings to humans may be difficult due to species-specific expression pattern of circRNAs. In future studies, we will use a human *in vitro* model of hypoxia to verify that the dysregulation of candidate circRNAs is conserved between species. Second, translating the findings to the clinic may prove problematic due to the lack of rapid and easy detection of circRNAs associated with PWMD. Thus, we will obtain information on the expression profiles of circRNAs from the plasma and serum of PWMD and control rats and premature infants, and select circRNAs for functional and mechanic studies.

Conclusion

We showed that circRNAs are dysregulated in the brains of rats with PWMD compared with sham rats. These findings may provide preliminary data that can be used to identify candidate for PWMD diagnosis, and insight into the mechanisms of PWMD.

Acknowledgements

This project was supported by grants from the National Natural Science Foundation of China (nos. 81601355 and 81771628) and the Natural Science Foundation of Jiangsu Health Vocational College (JKA201705).

Disclosure Statement

The authors have no conflicts of interest to disclose. The authors have no financial relationships relevant to this article to disclose.

References

1 Volpe JJ: Neurology of the Newborn, ed 4. Philadelphia: WB Saunders, 2001.
2 Johnson S, Marlow N: Positive screening results on the modified checklist for autism in toddlers: Implications for very preterm populations. J Pediatr 2009;154:478-480.
3 Larroque B, Ancel PY, Marret S, Marchand L, Andre M, Arnaud C, Pierrat V, Roze JC, Messer J, Thiriez G, Burguet A, Picaud JC, Breart G, Kaminski M: Neurodevelopmental disabilities and special care of 5-year-old children born before 33 weeks of gestation (the EPIPAGE study): A longitudinal cohort study. Lancet 2008;371:813-820.
4 Liu XB, Shen Y, Plane JM, Deng WB: Vulnerability of premyelinating oligodendrocytes to white-matter damage in neonatal brain injury. Neurosci Bull 2013;29:229-238.
5 Volpe JJ: Brain injury in premature infants: A complex amalgam of destructive and developmental disturbances. Lancet Neurol 2009;8:110-124.
6 Chen HJ, Wei KL, Zhou CL, Yao YJ, Yang YJ, Fan XF, Gao XR, Liu XH, Qian JH, Wu BQ, Wu GQ, Zhang QM, Zhang XL: Incidence of brain injuries in premature infants with gestational age a parts per thousand currency sign34 weeks in ten urban hospitals in China. World J Pediatr 2013;9:17-24.
7 Rink C, Khanna S: MicroRNA in ischemic stroke etiology and pathology. Physiol Genomics 2011;43:521-528.
8 Zhao F, Qu Y, Liu J, Liu H, Zhang L, Feng Y, Wang H, Gan J, Lu R, Mu D: Microarray profiling and Co-Expression network analysis of LncRNAs and mRNAs in neonatal rats following hypoxic-ischemic brain damage. Sci Rep 2015;5:13850.
9 Lu D, Xu AD: Mini review: Circular RNAs as potential clinical biomarkers for disorders in the central nervous system. Fron Genet 2016;7:53.
10 Conn SJ, Pillman KA, Toubia J, Conn VM, Salmanidis M, Phillips CA, Roslan S, Schreiber AW, Gregory PA, Goodall GJ: The RNA binding protein quaking regulates formation of circRNAs. Cell 2015;160:1125-1134.
11 Lasda E, Parker R: Circular RNAs: Diversity of form and function. RNA 2014;20:1829-1842.
12 Chen I, Chen CY, Chuang TJ: Biogenesis, identifcation, and function of exonic circular RNAs. Wiley Interdiscip Rev RNA 2015;6:563-579.
13 Memczak S, Jens M, Elefsinioti A, Torti F, Krueger J, Rybak A, Maier L, Mackowiak SD, Gregersen LH, Munschauer M, Loewer A, Ziebold U, Landthaler M, Kocks C, le Noble F, Rajewsky N: Circular RNAs are a large class of animal RNAs with regulatory potency. Nature 2013;495:333-338.
14 Chen LL, Yang L: Regulation of circRNA biogenesis. RNA Biol 2015;12:381-388.
15 Suzuki H, Tsukahara T: A view of pre-mRNA splicing from RNase R resistant RNAs. Int J Mol Sci 2014;15:9331-9342.
16 Hansen TB, Jensen TI, Clausen BH, Bramsen JB, Finsen B, Damgaard CK, Kjems J: Natural RNA circles function as efficient microRNA sponges. Nature 2013;495:384-388.
17 Westholm JO, Miura P, Olson S, Shenker S, Joseph B, Sanfilippo P, Celniker SE, Graveley BR, Lai EC: Genome-wide analysis of drosophila circular RNAs reveals their structural and sequence properties and age-dependent neural accumulation. Cell Rep 2014;9:1966-1980.
18 Rybak-Wolf A, Stottmeister C, Glazar P, Jens M, Pino N, Giusti S, Hanan M, Behm M, Bartok O, Ashwal-Fluss R, Herzog M, Schreyer L, Papavasileiou P, Ivanov A, Ohman M, Refojo D, Kadener S, Rajewsky N: Circular RNAs in the mammalian brain are highly abundant, conserved, and dynamically expressed. Mol Cell 2015;58:870-885.
19 Szabo L, Morey R, Palpant NJ, Wang PL, Afari N, Jiang C, Parast MM, Murry CE, Laurent LC, Salzman J: Statistically based splicing detection reveals neural enrichment and tissue-specific induction of circular RNA during human fetal development. Genome Biol 2015;16:126.
20 Gruner H, Cortes-Lopez M, Cooper DA, Bauer M, Miura P: CircRNA accumulation in the aging mouse brain. Sci Rep 2016;6:38907.
21 Chen W, Schuman E: Circular RNAs in brain and other tissues: A functional enigma. Trends Neurosci 2016;39:597-604.
22 Hansen TB, Kjems J, Damgaard CK: Circular RNA and miR-7 in cancer. Cancer Res 2013;73:5609-5612.
23 Wan L, Zhang L, Fan K, Cheng ZX, Sun QC, Wang JJ: Circular RNA-ITCH suppresses lung cancer proliferation via inhibiting the Wnt/beta-Catenin pathway. Biomed Res Int 2016;2016:1579490.

24 Barbagallo D, Caponnetto A, Cirnigliaro M, Brex D, Barbagallo C, D'Angeli F, Morrone A, Caltabiano R, Barbagallo GM, Ragusa M, Di Pietro C, Hansen TB, Purrello M: CircSMARCA5 Inhibits Migration of Glioblastoma Multiforme Cells by Regulating a Molecular Axis Involving Splicing Factors SRSF1/SRSF3/PTB. Int J Mol Sci 2018;19:E480.
25 Qian Y, Lu Y, Rui C, Qian Y, Cai M, Jia R: Potential significance of circular RNA in human placental tissue for patients with preeclampsia. Cell Physiol Biochem 2016;39:1380-1390.
26 Boeckel JN, Jaé N, Heumüller AW, Chen W, Boon RA, Stellos K, Zeiher AM, John D, Uchida S, Dimmeler S: Identification and Characterization of Hypoxia-Regulated Endothelial Circular RNA. Circ Res 2015;117:884-890.
27 Boeckel JN, Jaé N, Heumüller AW, Chen W, Boon RA, Stellos K, Zeiher AM, John D, Uchida S, Dimmeler S: Screening circular RNA expression patterns following focal cerebral ischemia in mice. Oncotarget 2017;8:86535-86547.
28 Zhu L, Bai X, Wang S, Hu Y, Wang T, Qian L, Jiang L: Recombinant human erythropoietin augments angiogenic responses in a neonatal rat model of cerebral unilateral Hypoxia-Ischemia. Neonatology 2014;106:143-148.
29 Gao Y, Wang J, Zhao F: CIRI: An efficient and unbiased algorithm for de novo circular RNA identification. Genome Biol 2015;16:4.
30 Li H: Aligning sequence reads, clone sequences and assembly contigs with BWA-MEM. Quantitative Biology 2013.
31 Kent WJ, Sugnet CW, Furey TS, Roskin KM, Pringle TH, Zahler AM, Haussler D: The human genome browser at UCSC. Genome Res 2002;12:996-1006.
32 Salzman J, Chen RE, Olsen MN, Wang PL, Brown PO: Cell-type specific features of circular RNA expression. Plos Genet 2013;9:e1003777.
33 You X, Vlatkovic I, Babic A, Will T, Epstein I, Tushev G, Akbalik G, Wang M, Glock C, Quedenau C, Wang X, Hou J, Liu H, Sun W, Sambandan S, Chen T, Schuman EM, Chen W: Neural circular RNAs are derived from synaptic genes and regulated by development and plasticity. Nat Neurosci 2015;18:603-610.
34 Liu YC, Li JR, Sun CH, Andrews E, Chao RF, Lin FM, Weng SL, Hsu SD, Huang CC, Cheng C, Liu CC, Huang HD: CircNet: A database of circular RNAs derived from transcriptome sequencing data. Nucleic Acids Res 2016;44:D209-D215.
35 Huang DW, Sherman BT, Lempicki RA: Systematic and integrative analysis of large gene lists using DAVID bioinformatics resources. Nat Protoc 2009;4:44-57.
36 Huang DW, Sherman BT, Tan Q, Kir J, Liu D, Bryant D, Guo Y, Stephens R, Baseler MW, Lane HC, Lempicki RA: DAVID Bioinformatics Resources: Expanded annotation database and novel algorithms to better extract biology from large gene lists. Nucleic Acids Res 2007;35:W169-W175.
37 Wu J, Mao X, Cai T, Luo J, Wei L: KOBAS server: A web-based platform for automated annotation and pathway identification. Nucleic Acids Res 2006;34:W720-W724.
38 Liu Q, Zhang X, Hu X, Dai L, Fu X, Zhang J, Ao Y: Circular RNA Related to the Chondrocyte ECM Regulates MMP13 Expression by Functioning as a MiR-136 'Sponge' in Human Cartilage Degradation. Sci Rep 2016;6:22572.
39 Liu XB, Shen Y, Pleasure DE, Deng W： The vulnerability of thalamocortical circuitry to hypoxic-ischemic injury in a mouse model of periventricular leukomalacia. BMC Neurosci 2016;17:2.
40 Yan F, Zhang M, Meng Y, Li H, Yu L, Fu X, Tang Y, Jiang C: Erythropoietin improves hypoxic-ischemic encephalopathy in neonatal rats after short-term anoxia by enhancing angiogenesis. Brain Res 2016;1651:104-113.
41 Qu S, Yang X, Li X, Wang J, Gao Y, Shang R, Sun W, Dou K, Li H: Circular RNA: A new star of noncoding RNAs. Cancer Lett 2015;365:141-148.
42 Chen LL, Yang L: Regulation of circRNA biogenesis. Ran Biol 2015;12:381-388.
43 Jeck WR, Sorrentino JA, Wang K, Slevin MK, Burd CE, Liu J, Marzluff WF, Sharpless NE: Circular RNAs are abundant, conserved, and associated with ALU repeats. RNA 2013;19:141-157.
44 Li F, Zhang L, Li W, Deng J, Zheng J, An M, Lu J, Zhou Y: Circular RNA ITCH has inhibitory effect on ESCC by suppressing the Wnt/beta-catenin pathway. Oncotarget 2015;6:6001-6013.
45 Zhang Y, Zhang XO, Chen T, Xiang JF, Yin QF, Xing YH, Zhu S, Yang L, Chen LL: Circular intronic long noncoding RNAs. Mol Cell 2013;51:792-806.

46 Li Z, Huang C, Bao C, Chen L, Lin M, Wang X, Zhong G, Yu B, Hu W, Dai L, Zhu P, Chang Z, Wu Q, Zhao Y, Jia Y, Xu P, Liu H, Shan G: Exon-intron circular RNAs regulate transcription in the nucleus. Nat Struct Mol Biol 2015;22:256-264.
47 You X, Vlatkovic I, Babic A, Will T, Epstein I, Tushev G, Akbalik G, Wang M, Glock C, Quedenau C, Wang X, Hou J, Liu H, Sun W, Sambandan S, Chen T, Schuman EM, Chen W: Neural circular RNAs are derived from synaptic genes and regulated by development and plasticity. Nat Neurosci 2015;18:603-610.
48 Li P, Chen S, Chen H, Mo X, Li T, Shao Y, Xiao B, Guo J: Using circular RNA as a novel type of biomarker in the screening of gastric cancer. Clin Chim Acta 2015;444:132-136.
49 Wang Z, Gerstein M, Snyder M: RNA-Seq: A revolutionary tool for transcriptomics. Nat Rev Genet 2009;10:57-63.
50 Hansen TB, Veno MT, Damgaard CK, Kjems J: Comparison of circular RNA prediction tools. Nucleic Acids Res 2016;44:e58.
51 Jeck WR, Sharpless NE: Detecting and characterizing circular RNAs. Nat Biotechnol 2014;32:453-461.
52 Wu HJ, Zhang CY, Zhang S, Chang M, Wang HY: Microarray expression profile of circular RNAs in heart tissue of mice with myocardial Infarction-Induced heart failure. Cell Physiol Biochem 2016;39:205-216.
53 Peng L, Yuan XQ, Li GC: The emerging landscape of circular RNA ciRS-7 in cancer. Oncol Rep 2015;33:2669-2674.
54 Fan X, Heijnen CJ, van der Kooij MA, Groenendaal F, van Bel F: The role and regulation of hypoxia-inducible factor-1alpha expression in brain development and neonatal hypoxic-ischemic brain injury. Brain Res Rev 2009;62:99-108.
55 Lu J, Jiang L, Zhu H, Zhang L, Wang T: Hypoxia-inducible factor-1alpha and erythropoietin expression in the hippocampus of neonatal rats following hypoxia-ischemia. J Nanosci Nanotechnol 2014;14:5614-5619.
56 Zheng Q, Bao C, Guo W, Li S, Chen J, Chen B, Luo Y, Lyu D, Li Y, Shi G, Liang L, Gu J, He X, Huang S: Circular RNA profiling reveals an abundant circHIPK3 that regulates cell growth by sponging multiple miRNAs. Nat Commun 2016;7:11215.